Molecular Crystals and Liquid Crystals Science and Technology. Section A. Molecular Crystals and Liquid Crystals

Publication details, including instructions for authors and subscription information:
http://www.tandfonline.com/loi/gmcl19

Molecular and Atomic Arrays in Nano- and Mesoporous Materials Synthesis

G. D. Stucky [a], A. Monnier [a], F. Schüth [a], Q. Huo [a], D. Margolese [a], D. Kumar [a], M. Krishnamurty [b], P. Petroff [b], A. Firouzi [c], M. Janicke [c] & B. F. Chmelka [c]

[a] Department of Chemistry, University of California, Santa Barbara, California, 93106, U.S.A.

[b] Materials Department, University of California, Santa Barbara, California, 93106, U.S.A.

[c] Department of Chemical and Nuclear Engineering, University of California, Santa Barbara, California, 93106, U.S.A.

Version of record first published: 24 Sep 2006.

To cite this article: G. D. Stucky , A. Monnier , F. Schüth , Q. Huo , D. Margolese , D. Kumar , M. Krishnamurty , P. Petroff , A. Firouzi , M. Janicke & B. F. Chmelka (1994): Molecular and Atomic Arrays in Nano- and Mesoporous Materials Synthesis, Molecular Crystals and Liquid Crystals Science and Technology. Section A. Molecular Crystals and Liquid Crystals, 240:1, 187-200

To link to this article: http://dx.doi.org/10.1080/10587259408029730

Mol. Cryst. Liq. Cryst. 1994, Vol. 240, pp. 187–200
Reprints available directly from the publisher
Photocopying permitted by license only

Printed in the United States of America

Molecular and Atomic Arrays in Nano- and Mesoporous Materials Synthesis

G. D. Stucky†, A. Monnier†, F. Schüth†, Q. Huo†, D. Margolese†, D. Kumar†, M. Krishnamurty§, P. Petroff§, A. Firouzi‡, M. Janicke‡ and B.F. Chmelka‡
†Department of Chemistry, §Materials Department and ‡Department of Chemical and Nuclear Engineering, University of California, Santa Barbara, California, 93106, U.S.A.

Abstract A model is presented to explain the formation and morphologies of 3-d periodic surfactant-silicate mesostructures. The structures of lamellar, hexagonal tubular and a minimal surface cubic liquid crystal/silicate phase are described.

INTRODUCTION

The ideal 3-d nanocomposite has precise size and topographical definition of nanophases; a 3-d supra-lattice periodicity; and, tunability with respect to topography, nanophase dimensions, intra-phase interactions, and surface states defined by the inter - phase interfaces. One approach to synthetically achieving these goals is to use 3-d substrate surfaces, where the 3-d surfaces are defined by periodic arrays of channels and/or cages. Nano dimensioned porous materials such as zeolites have their origins in single molecule template synthesis and have effective channel size kinetic diameters of < 15 Å. Catalytic reactions and separations of small molecules with dimensions which are within this size regime can be carried out with an extremely high degree of selectivity which is determined by both stearic and adsorption processes on the very high area substrate. From a materials standpoint, the self-organization of organic molecules within these nano-sized channels provides an opportunity to study nucleation and self assembly phenomena ranging from mono, bi to polymolecular strands as defined by the guest molecular dimensions[1].

Mesoporous (15 - 500 Å) materials with a regular 3-d periodicity and high surface areas have potential use in biotechnology applications, chemical sensors, large molecule selective catalysis (including heavy crude oil processing) and as highly ordered matrix for optical data storage and quantum confinement devices. In order to create ordered pores of these dimensions analogous to those found in zeolites, a larger templating surface must be provided during synthesis. Attempts to create a building block by templating around a large molecule have had limited success and to date not proven to be a way to systematically extend pore/channel dimensions beyond 12-13 Å. An alternative

challenging and potentially more rewarding approach for the synthesis of meso - dimensioned porous media is to utilize organized molecular arrays as templates for the condensation of the inorganic phase[2]. Synthetically the goal is to kinetically and thermodynamically interface the self assembly of an organic amphiphilic array with the polymerization of an inorganic phase of controlled thickness into a 3-d porous network. Three types of assembly (amphophile, inorganic polymer and interface) must occur simultaneously in the same synthesis media since unlike 2-d superlattice syntheses the 3–d zeolitic pore periodicity can not be achieved by the sequential synthesis of planar layers of alternating organic and inorganic composition.

Pores of this dimension in principal could serve as scaffolding for biocatalysis or molecular recognition processes by attaching appropriate molecular units directly to the pore walls since these the large pore dimensions would still permit molecular diffusion through the functionalized channels. A second goal in the synthesis of mesoporous cage and channel surfaces is therefore to be able to functionalize the appropriate host framework with molecular fragments attached to the pore walls and thus structure direct the assembly and selective absorption of other guest molecules.

LIQUID CRYSTAL AND INORGANIC MESOPHASE INTERFACE CHEMISTRY

Lamellar, cubic and hexagonal mesopore silicate phases have been recently prepared by direct synthesis using $(CH_3)_3N^+(C_nH_{2n+1})\ X^-$ (n = 10 to 30) liquid crystal arrays and soluble silica sources[2]. Our interest has been to develop a synthesis model which will explain presently known experimental data and successfully extend organized molecular array/inorganic interface chemistry to the general synthesis of silicate and non siliceous mesostructure materials.

Physically several fundamental processes must be considered: 1) self organization of the amphiphilic molecules, 2) inorganic phase condensation, 3) the interface chemistry between silicate and liquid crystal phases and 4) assembly of adjacent surfactant/silicate arrays to generate long range 3-d periodicity. These can be summarized in terms of the Gibbs free energy as follows:

$$G = G_{intra}(A, ...) + G_{polysil}(\rho, ...) + G_{inter}(A, \rho, ...) + G_{sol} \qquad (1)$$

In this representation A = area per $(CH_3)_3N^+$ head group with an optimal value A_0 obtained by minimizing the free energy, G (i.e. $A_0 \rightarrow (\partial G/\partial A) = 0$). ρ = a generic variable representing the state of the wall by specifying the distribution of the various

species within it. The wall charge and thickness are defined by ρ. $G_{intra}(A, ...)$ results from the van der Waals forces and conformational energy of the hydrocarbon chains and the van der Waals and electrostatic interactions of the head groups within a single micelle or liquid crystal phase. $G_{polysil}(\rho, ...)$ reflects the contribution arising from the inorganic wall. This is a measure of the polysilicate structural free energy, including the solvent, counterion, and silicate van der Waals and electrostatic interactions within the inorganic silicate framework or "wall". $G_{inter}(A, \rho, ...)$ accounts for the van der Waals and electrostatic effects associated with inter silicate/surfactant array interactions and surfactant-silicate wall interactions. G_{sol} = contribution of the mother liquor solution. This contribution sets the chemical potential of the various species within the precipitate.

The approach that we have taken is to consider the synthesis phase space and the properties of the lamellar, hexagonal and cubic mesophases in the context of the above description, i.e. the interface chemistry of two phase-separated organic and inorganic arrays. In this paper, studies of the synthesis, structural and chemical functionalization properties of selected mesoporous silicate phases synthesized using liquid crystal arrays as templates are first described[3]. The last section relates these results to a mechanistic model for biphasic mesostructure synthesis using organized molecular arrays as templates.

SYNTHESIS

In order to identify conditions important for the formation of mesoporous materials, syntheses were performed over a wide range of starting materials, compositions and temperatures. Aqueous solutions were used over a temperature range of 25 °C to 170 °C in open beaker, reflux or autoclave environments. The silica sources used included sodium silicate, fumed silica, colloidal silica (Ludox), tetraethoxysilicate (TEOS), tetramethylammonium silicate and elementary silicon. The aluminum sources consisted of boehmite or sodium aluminate. Phosphoric acid and the appropriate metal nitrate or metal alkoxide were used in the synthesis of metal phosphate phases. A variety of surfactants were examined, but the work reported here used $C_nH_{2n+1}N(CH_3)_3X$ (n = 8 to 24, X = Cl^-, Br^-, OH^-). NaOH and $(CH_3)_4NOH$ were used as bases. The swelling agents used in the synthesis were 1,3,5-trimethylbenzene and ethyl benzene. In general the procedure was to stir the basic silica solution into the surfactant/swelling agent/alumina solution, using a stirred autoclave reactor and autogenous pressures as appropriate. The pore diameter can be systematically changed by either changing the length of the surfactant chain or by inclusion of the swelling agent into the surfactant organic region. The pore

diameter increases nearly linearly with the swelling agent concentration up to the limit of its solubility.

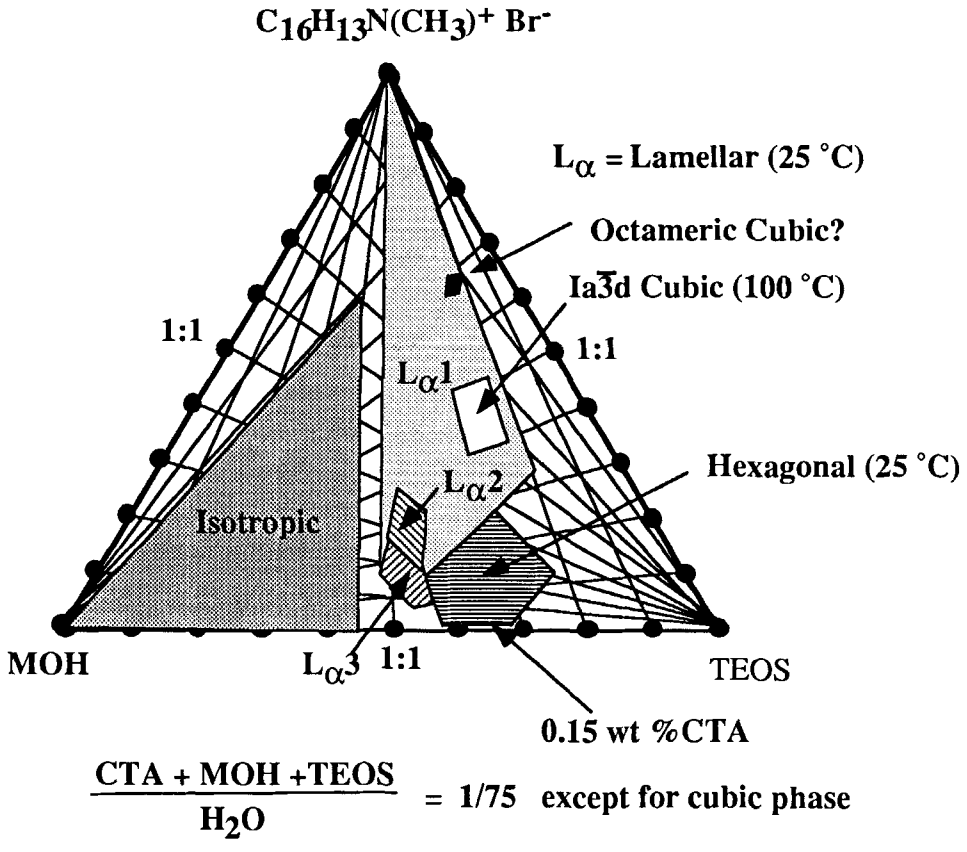

Figure 1 Synthesis space diagram of silicate mesostructures. Reactions were carried out at room temperature except for the cubic phases which were done at 100 °C.

Two regions of the synthesis space of particular interest to us for this investigation were at low surfactant concentrations and low temperatures (25 to 100 °C). It is possible to slow the evolution of the surfactant-silicate systems and isolate intermediate phases which were previously unreported in both of these regions. Moreover, we were able to obtain silicate mesostructure materials (Figure 1) under conditions where the silicate alone would not condense (e.g. silicate concentrations of 0.5 to 5% and room temperature at pH's between 12 and 14) nor would the surfactant alone form a liquid crystal phases. For example, only isotropic micelle phases are present in the CTABr-water phase diagram at trimethylammonium (CTA) concentrations < 1%, yet hexagonal surfactant-silicate phases

are readily formed under these conditions at room temperature. For a CTABr-water solution at typical surfactant-synthesis temperatures in the absence of silicates, a hexagonal phase is favored at surfactant concentrations from ~ 25 to 70% by weight, while cubic and lamellar phases form at concentrations above 70%.[4] An interesting variation on the isotropic → hexagonal → cubic → lamellar sequence is observed for lamellar and hexagonal surfactant/silicate mesostructures as noted in the following discussion on the lamellar phases.

LAMELLAR PHASES

Four distinct lamellar phases have been observed, all with repeat distances between 26 Å and 36 Å using CTA as the surfactant. One of these is the pure lamellar phase of CTA (26.0 Å). The variation of the d-spacing as a function of the chain length of the cationic surfactant has been determined to be 1.0 to 1.2 Å/carbon, and clearly indicates an interdigitated monolayer assembly. For silicate compositions the layers are turbostratic (no observed lateral ordering between layers) with only (00l), l = 1-3 or 4 reflections being observed. This is to be contrasted with the zinc phosphate layered structures obtained through synthesis with the same templates which show excellent registry between layers and also an interdigitated monolayer liquid crystal assembly.

During freeze-dry kinetic experiments using CTABr as the surfactant, a lamellar phase with a primary d-spacing of 31 (± 1) was formed together with amorphous silica, after reaction times on the order of 1 minute. The lamellar phase disappears after about 20 minutes, at which point the hexagonal phase is simultaneously detected. The hexagonal phase reaches its final crystallinity after ~10 hours and has a primary d-spacing of 40 (± 1) Å. A lamellar phase with the same primary d-spacing of 31 (± 1) Å can be isolated in pure form and also converted to the hexagonal mesoporous phase within 10 days if hydrothermally treated at 373 °K (pH = 7). The same transformation can also be observed by in situ X-ray diffraction studies beginning with the wet lamellar phases. ^{29}Si MASNMR experiments show that during this transformation the degree of polymerization increases with the Q_3/Q_4 ratio[5] decreasing from typical values of 1 (lamellar) to 0.5 (hexagonal). The only anion present by chemical analysis is the silicate so that this change in Q_3/Q_4 ratio is also a measure of the change in the silicate wall charge during the transformation from lamellar to hexagonal phase.

HEXAGONAL PHASE

TEM electron diffraction and lattice imaging clearly shows two dimensional ordering of the hexagonal phase (hki0 reflections), consistent with a hexagonal array of parallel silicate tubes. The unit cell parameter is then equal to the dimensions of a pore and one pore wall thickness. X-ray diffraction gives a total of 5 to 6 diffraction peaks which are still present after calcination in N_2/O_2 at temperatures as high as 850 °C to remove the organic guest phase. The primary [hkil = (1000)] Bragg reflection was observed after calcination at 1200 °C, although the other higher order reflections were no longer present. Neither X-ray diffraction or tilted stage electron diffraction gave any indication of ordering parallel to the tube walls. FTIR and Raman spectroscopy confirmed at least the partial disorder of the silicate groups within the tube walls.

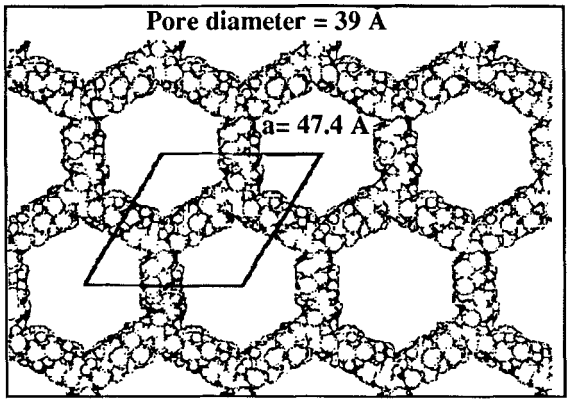

Figure 2 Hexagonal phase silicate mesopore model. Pore size can be varied with 1,3,5 trimethylbenzene/surfactant concentration.

Using these results, the X-ray data for the calcined structure were fit to a model which assumed an amorphous continuous scatterer for the wall, and a periodic hexagonal array of void tubes. Two parameters were refined, the wall thickness and the pore shape, by using analytically derived functions to describe cylindrical and hexagonal geometries as wall shape functions. This analysis gives a wall thickness of 8 (± 1) Å for unit cells varying between 37.5 and 46.9 Å and a best fit for hexagonal shaped pores. The corresponding void space fraction varies from 0.6 to 0.7 which is in excellent agreement with BET void space (Ar and N_2) of 0.62 to 0.74 for unit cells between 30 and ~100 Å, and benzene uptake measurements which gave 0.63 for the void space of a 35 Å unit cell. The pore wall thickness of 8 (± 1) Å strongly implies that the wall structure is made up of two silicate monolayers (Figure 2).

It is of interest to analyze these results with a geometrical constant volume model describing the layered to hexagonal phase transformation using the CTABr data reported for this transition for the pure phase by Husson, et al [6]. The model inter-relates surfactant partial volume, silicate or electrolyte wall thickness and interface head group area (A in equation 1 above) to the observed hexagonal and layer d spacings. This analysis gives wall thicknesses of 8.95 Å and 10.85 Å for the hexagonal and layered silicate

mesostructure phases respectively. More interestingly, the interface surfactant head group area is smaller for the lamellar phase (59.7 Å ^{2}) than for the hexagonal phase (67.1 Å ^{2}), consistent with the higher charge density expected for a surface of lower curvature (lamellar phase). The corresponding wall thickness for the pure liquid crystal surfactant phases are 5.8 and 5.7 Å for the lamellar and hexagonal phases, while the lamellar phase surfactant head group area is also smaller (42.8 Å ^{2}) compared to that of the hexagonal phase (60.5 Å ^{2}).

The structure of the mesophase walls has been studied in detail by FTIR, thermal analysis, Raman spectroscopy, ^{1}H and ^{29}Si, and prompt gamma analysis using silylation with trimethylsilylchloride on hexagonal phase samples which have had the organic liquid crystal removed at low temperatures by reflux in acid/organic solvents. These data show that one half of the wall silicon atoms of the as synthesized hexagonal phase have terminal oxygen or hydroxyl groups. Of these ~50% are pore accessible and can be readily functionalized by silylation[7].

CUBIC PHASE

The Ia3d MCM-48 cubic phase was synthesized with C_{12}, C_{14}, and C_{16} micelles and structurally characterized using as many as 17 observable and indexable X-ray lines. The phase was clean with no evidence of auxiliary phases. X-ray modelling of the CTA cubic phase X-ray data similar to that described above for the hexagonal phase X-ray data has given an excellent fit for the Q^{230} model proposed by Mariani et al [8] for water surfactant systems. This model can also be described by a gyroid periodic minimal surface (g surface). A periodic minimal surface by definition is the smallest surface separating a volume into two equal parts given a certain periodic constraint[9]. This structure can then be viewed as a single infinite silicate sheet separating the surfactant species into two equal and disconnected volumes. This is a bicontinuous surface with two non-intersecting pore arrays, each of which however has intersecting pores.

MESOSTRUCTURE ASSEMBLY: MICELLES + SILICATE POLYMERIZATION

We consider here a possible mechanism for silicate mesostructure synthesis in the context of equation (1). If the final mesophase morphology depended solely on the surfactant concentration, the lamellar silica phase would be found at the highest, cubic at next highest and hexagonal phase at the lower surfactant concentrations. Below surfactant concentrations of ~20 wt % an isotropic micelle geometry is expected between room

temperature and 80 °C. Higher temperatures and higher concentrations would favor the lamellar mesophase.

Surfactant concentrations used in the syntheses reported here are between 0.15% and 30%. In at least one region of the synthesis phase space the lamellar phase is a precursor phase to the hexagonal phase as a function of the silicate condensation time. The observation of a hexagonal surfactant/silicate phase at surfactant concentrations as low as 0.15% is also inconsistent with the pure surfactant phase diagram. These data indicate that the silicate phase is structurally determining the liquid crystal array morphology. Qualitatively, however, the shape and size resemblance of the silicate mesophase to the corresponding surfactant liquid crystal structures suggest that the interactions responsible for the final mesophase morphology must be similar to that for the surfactant.

$G_{intra}(A, ...)$

The structure directing role of the head group area (A) in the selection of particular mesophase has been recognized in water-surfactant systems. The preferred mesophase is that which permits the surfactant head group area to be closest to its optimal value, Ao, with favorable packing of the hydrophobic surfactant chains. Israelachvili and Chavrolin and Srdoc have proposed a simple dimensionless packing parameter $g = V/A_0l_c = A_t/A_0$ to determine the preferred shape of the surfactant liquid crystal[10]. V is the hydrocarbon tail volume, l_c is the length of the hydrocarbon chain and A_0 is the optimal average area of the hydrocarbon chain projected along the chain axis. Spherical micelles form if $g < 1/3$, cylindrical micelles occur for $1/3 < g < 1/2$, vesicles or bilayer for $1/2 < g < 1$ and inverted micelles for $g > 1$. Consistent with this packing parameter, we do not observe short chain ($n < 16$) pure silica phase lamellar structures which have a small value for A_t at low synthesis temperatures. On the other hand at high temperatures or for long hydrocarbon chains which have a large A_t, the lamellar silicate structure is found.

As the surfactant concentration is increased, the anion charge concentration for a fixed water volume increases within the water layers which form the walls that separate the head groups. A_0 then decreases because of the increased anionic charge per unit "wall" volume, and the higher charge density liquid crystal surface, lamellar, becomes the preferred morphology.

$G_{polysil}(\rho, ...)$

An intriguing aspect of the above experimental NMR data is that as the silicate condenses, its charge,ρ_ε, is decreasing. We suggest that this dynamic change in charge density is responsible for the lamellar $\rightarrow$ hexagonal transition observed during synthesis

(see below). At the pH used in the synthesis (9 to 14), monomeric or dimeric silicates (pK_a = 9.8 and 10.7)[11] are only slightly dissociated under the conditions employed here. However, small silica oligomers (3-7 Si atoms) of varying degree of polymerization and charge are also present at high pH[12]. On the other hand oligomers are appreciable more acidic (pKa ~ 6.5) and are close to 100% ionized at the synthesis pH.

The first consequence of the above chemical considerations is that neutral monomeric or dimeric species without charge can condense relatively easily to give charged silicate oligomers. Furthermore, while monovalent monomers or dimers such as $Si(OH)_3O^-$ have no energetic advantage over other anions competing for access to the surfactant cationic head groups, the oligomeric silica polyanions can easily act as multidentate ligands for the cationic head groups of the surfactant, leading to a strongly interacting surfactant-silicate interface. This free energy contribution also contain the structural constraints responsible for the multidentate binding. It is particularly important to note that the silicate portion of the mesostructure has its highest negative charge at the earliest stages of synthesis. This charge decreases with subsequent polymerization and condensation of the silicate "skin" on the liquid crystal surface. When the liquid crystal arrays are removed from the silicate framework at low temperatures by reflux in an acidic ether solution which also protonates the available nonbridging oxygen atoms, the NMR and silylation data show that the silicate tetrahedra have an "up - down" disorder within the silicate monolayers with 50% of the Q_3 sites being intra-wall sites. These intra-wall sites are at the interface of two condensing silicate monolayer surfaces on adjacent micelle arrays and contribute to the interarray interactions which are part of $G_{inter}(A, \rho, ...)$.

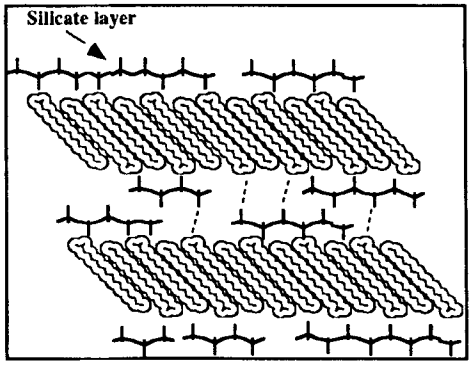

Figure 3 Schematic of early stages of silicate oligomer condensation on liquid crystal array. Dashed lines indicate electrostatic inter-array interactions.

$G_{inter}(A, \rho, ...)$

Preferential multidentate binding of the charged surfactant and silicate species is a highly favored thermodynamic process and is undoubtedly the fast step in the synthesis process. It explains why it is possible to form silicate mesostructures even at room temperature with very low surfactant concentrations. The surfactant surface is quickly

populated by silicate oligomers, which only subsequently polymerize further in a relatively slow step process. Phase precipitation of the surfactant-silicate system is primarily the result of electrostatic interactions combined with packing constraints associated with the hydrophobic surfactant chain. It also must involve interarray electrostatic interactions, perhaps as a result of incomplete or inhomogeneous coverage of a given surfactant array by the silicate fragments (Figure 3). In any event, precipitation is fast and thermodynamically controlled.

Silica polymerization and the ultimate synthesis of a strong and extended framework is slow and reaction limited. This polymerization within the liquid crystal-silicate interface is nevertheless favorable because 1) the concentration of silicate species near the interface is high; and 2) their negative charges are partially screened by the surfactant. As the polymerization proceeds, the generation of highly connected silicate polyanions which act as very large multidentate ligands further enhances the cooperative binding between the surfactant and silicate species, even though the silicate charge is decreasing to a limiting value with condensation as found experimentally for the hexagonal wall structure.

This two stage process agrees with our experimental findings concerning the differences in mesostructures formed at room temperature after short reaction times with those obtained at high temperature after long reaction times. Both have very similar X-ray patterns and apparently identical mesostructures, however the low temperature phases are thermally, hydrolytically and mechanically much less stable when compared to the high temperature phase. Calcination at elevated temperatures (550 °C) is another way of expediting the silica polymerization, giving a Q_3/Q_4 ratio of ~0.15 and terminal oxygen atoms which are all accessible through the pores and can be silylated.

The observed periodicity of the wall structure in the observed mesostructures indicates that the silicate wall thickness is precisely mediated during the assembly process. The wall thickness of the hexagonal phase is constant (8-9 Å) over wide reaction conditions independent of the surfactant chain length. The hexagonal pore shape maximizes the interface interaction between surfactant and silicate. Polymerization of silicate normal to the interface which would thicken the wall does not take place because of the strong electrostatic repulsion produced by the high negative charge on the silicate species at pH above 10.

The silicate wall must be thick enough to screen head group charges on either side of the silicate wall for a given surfactant/silicate charge ratio. G_{inter} defines the relationship between the state of the wall described by ρ, and the head group area A. In terms of the electrostatic interactions which most likely dominate, the average surfactant surface charge

density given by 1/A is mutually screened by the silicate charge density, ρ_ε. This electrostatic interaction thus links the optimal head group area, A_0, as defined by equation 1, with the silicate charge density, ρ_ε, a relationship which we refer to as "charge density matching". Such interdependent electrostatic effects have been previously shown to control the d-spacings of surfactant intercalates in different mica type silicates[13], and also invoked to explain the "self-replication" process of silica layers in purely inorganic systems[14].

The transition between the lamellar and hexagonal mesophases is readily explainable on the basis of these considerations. In the early stages of the synthesis, the presence of highly charged silica oligomers favor a small head-group area, A_0, and a surfactant surface with minimal curvature which in this case is the lamellar surfactant configuration. As rearrangement and polymerization of the silicate species takes place the anionic silicate charge density, ρ_ε, decreases so that the optimal head group area, A_0, increases, while the number of compensating cations decreases. Simultaneously, the wall thickness can decrease from its initial value without energy cost, because the repulsive cation-cation interactions across the wall decrease. Since the silicate wall is poorly condensed during early stages of the synthesis, the system can increase its optimal head group area, A_0, by increasing the effective curvature of the liquid crystal surface, in this case adopting the hexagonal structure. Under these circumstances the wall thickness simultaneously decreases to keep the volume ratio CTA/silicate constant.

SOME PREDICTIONS

The above model predicts that the mesophase with the least curvature which is consistent with the surfactant, pH and silicate concentrations uses will form initially, e.g. the lamellar phase noted above. With silicate condensation the inorganic charge density decreases and lower surfactant charge densities (larger A_0) are needed, e.g. a hexagonal phase. The lamellar phase is not necessarily a precursor phase as it may not be the phase with the least curvature which is consistent with the surfactant concentration, pH, etc.

Consider the pure surfactant phase diagram from the perspective of the water phase. The biphase system consists of surfactant arrays with hydrophobic interiors and hydrophilic exteriors. The space between the surfactant arrays is filled with the aqueous phase. If the water content is large relative to the surfactant (small wall charge density), the isotropic and then the hexagonal phases are favored. As the water content decreases, the cubic and then the lamellar phases are preferred.

In the mesophase silicates, the intervening phase between the surfactant arrays is silicate instead of water. pH must now also be included in the phase diagram as it controls the wall charge density. At too low a pH, silicate polymerization occurs too rapidly relative to surfactant-silicate binding and an amorphous phase with variable thickness is expected without long range (interpore) periodicity. At relatively low hydroxyl anion concentrations the silicate species are less highly ionized and the silicate charge density is relatively low. In this pH regime, varying the surfactant to silicate (wall phase) ratio is analogous to varying the surfactant to water (wall phase) ratio in the pure micelle phase. Thus, beginning with small surfactant to silicate ratios, the preferred mesophase structures would be hex → cubic → lamellar. This picture is in the right direction with surfactant/TEOS concentration changes at a fixed MOH/H_2O concentration, e.g. the hexagonal phase is formed at the lowest surfactant: TEOS ratio, then the cubic and lamellar phases (Figure 1).

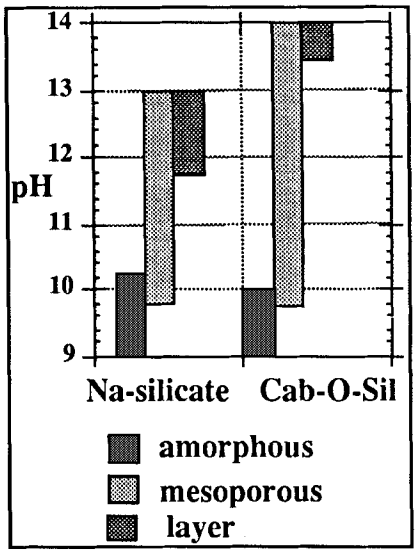

Figure 4 Phases obtained as a function of pH and silica source. Cab-O-Sil is made up of polymerized silica particles(100Å). Na-silicate refers to a solution of completely hydrolyzed silicates.

Increasing the pH increases the silicate ionicity and can be expected to increase the probability of obtaining lamellar structures and this is also observed (Figure 4). Similarly at the appropriate pH, a low degree of condensation of the silicate source can also be expected to favor the lamellar phases assuming incomplete redissolution of the more highly condensed and lower charge density silicate (Cab-O-Sil) reactant.

CONCLUSION

The synthesis of homogeneous nano and meso biphasic liquid crystal/inorganic composites with 3-d periodicity and pore structure requires chemical control at the atomic level of the self organization of the liquid crystal and inorganic phases, but is critically defined by the interface chemistry of the two phases and by interarray interactions. In order to be successful, it is necessary to match the thermodynamics and kinetics associated with these processes. The dynamics of this chemistry are well illustrated in silicate/liquid

crystal mesostructure synthesis by controlling the slow step of the synthesis, namely silicate condensation.

In this paper three specific key factors are identified to explain the formation and morphologies of surfactant-silicate mesostructures: multidentate binding of silicate oligomers to the cationic surfactant; preferential silicate polymerization in the interface region; and charge density matching between the surfactant and the silicate. The model explains current experimental data including a phase transition from lamellar to hexagonal phase and predicts the conditions favoring the formation of the lamellar, hexagonal and cubic mesophases in the context of water-surfactant liquid crystal systems. A cubic structure, Q^{230}, proposed by Mariani et al[8] satisfactorily fits the X-ray data collected on the cubic phase (a = 97 Å for CTA). This model suggests that the silicate polymer forms an unique infinite silicate sheet sitting on a gyroid minimal surface and separating the surfactant molecules in two disconnected volumes.

The extension of these concepts to other inorganic compositions and ordered organic arrays should provide the basis for the synthesis of a wide variety of new mesostructures and structural morphologies with long range periodic ordering and uniform, tunable pore geometries.

ACKNOWLEDGEMENTS

We thank J. Israelachvili (UCSB), J. Zasadzinski (UCSB), J. Beck (Mobil), J. Vartuli (Mobil), and J. Higgins (Mobil) for helpful discussions. The research was funded by the Office of Naval Research (GDS), NSF Science and Technology Center for Quantized Electronic Structures, DMR 91-20007 (GDS and PP), MRL Program of the National Science Foundation under award DMR 91-23048 (BFC and GDS), NSF New Young Investigator Program and the Camille and Henry Dreyfus Foundation (BFC), and through FNRS (AM) and DFG (FS) fellowships.

REFERENCES

1. (a) S.D. Cox, T.E. Gier, J.D. Bierlein and G.D. Stucky, J. Am. Chem. Soc., 110, 2986 (1988); (b) S.D. Cox, T.E. Gier, J.D. Bierlein and G.D. Stucky, Solid State Ionics, 32/33, 514 (1989); (c) A.L. Weisenhorn, J.E. MacDougall, S.A.C. Gould, S.D. Cox, W.S. Wise, J. Masie, P. Maivald, V.B. Elings, P.L. Hansma and G.D. Stucky, Science, 247, 1330 (1990); (d) S.D. Cox, T.E. Gier and G.D. Stucky, Chem. Mater., 2, 609 (1990); (e) S.D. Cox and G.D. Stucky, J. Phys. Chem., 95, 710 (1991).

2. (a) C.T. Kresge, M.E. Leonowicz, M.E. Roth, J.C. Vartuli, J.S. Beck, Nature, 359, 710 (1992); (b) J. S. Beck et al., J. Am. Chem. Soc., 114, 10834 (1992).

3. A. Monnier, F. Schüth, Q. Huo, D. Kumar, D. Margolese, G.D. Stucky, M. Krishnamurty, P. Petroff, A. Firouzi, M. Janicke and B.F. Chmelka, Science, in press, (1993).

4. (a) X. Auvray, C. Petipas, R. Anthore, I. Rico, A. Lattes, J. Phys. Chem., 93, 7458 (1989); (b) R. G. Laughlin, Surfactant Sci. Ser., 37, 1 (1991).

5. Q_3 is a measure of the number of silicon atoms with three Si-O-Si linkages and one terminal SI-O or SI-OH group. Q_4 corresponds to a fully condensed silicon atom with four Si-O-Si linkages.

6. F. Husson, H. Mustacchi and V. Luzzati, Acta Cryst., 13, 668 (1960).

7. D. Margolese and G. D. Stucky, submitted for publication, J. Chem. of Materials.

8. P. Mariani, V. Luzzati, and H. Delacroix, J. Mol. Biol., 204, 165 (1991).

9. See for example S. Andersson, S.T. Hyde, K. Larsson and S. Lidin, Chem. Rev., 88, 221 (1988).

10. (a) J. Chavrolin and J.F. Srdoc, J. Phys., 48, 189 (1987); (b) J.N. Israelachvili, Surfactants in Solution, Vol. 4, edited by K.L. Mittal and P. Bothorel, (Plenum, New York, 1987), p. 145.

11. R.K. Iler, The Chemistry of Silica (Wiley, New York, 1979), p. 182.

12. (a) R.K. Harris, C.T.G. Knight, W.E. Hull, ACS Symp. Ser. 194, 79 (1982); (b) C.T.G. Knight, R.G. Kirkpatrick, E. Oldfield, J. Mag. Reson., 78, (1988); (c) A.V. McCormick and A.T. Bell, Catal. Rev. Sci. Eng., 31, 97 (1989).

13. A. Weiss, Clays and Clay Minerals, Proceedings of the National Conference on Clays and Clay Minerals, 10, 191 (1961).

14. A. Weiss, Angew. Chem. Int. Ed. Engl., 20, 850 (1981).